'1991A&A...245..271A'

Astron. Astrophys. 245, 271–278 (1991)

ASTRONOMY AND ASTROPHYSICS

Particle acceleration inside a 'gas' of shock waves

A. Anastasiadis and L. Vlahos

Department of Physics, University of Thessaloniki, GR-54006 Thessaloniki, Greece

Received May 11, accepted October 9, 1990

Abstract. Multiple explosions, spherical shocks propagating inside an inhomogeneous medium or highly turbulent flows will form a large number of discontinuities moving randomly in space. We study the acceleration of ions and electrons in such an environment. *Our model is applied in solar flares* but our conclusions are independent of the details of the mechanism that forms the shock waves.

We find that for typical parameters of solar flares, a large number of ions ($\geq 10^{-2} n_0$, where n_0 is the ambient plasma density) with initial energy 200 KeV $\leq E_i \leq$ 1.2 MeV will be accelerated up to energies 20 to 60 MeV in less than 5 s. For the same parameters, electrons with initial energy 20 KeV $\leq E_i \leq$ 200 KeV are accelerated up to 5 MeV, in less than 1.5 s. We compared those results with the Fermi acceleration and found that Fermi process is slower and the energy gained much smaller.

The energy distribution of the accelerated particles *escaping* from the acceleration volume is of the form $f(E) \approx \exp(-E/T_h)$, where $T_{h_i} = 13$ MeV for the ions and $T_{h_e} = 1$ MeV for the electrons, for typical parameters (200 shock waves with velocities $2.5 \times V_A \leq V_s \leq 4 \times V_A$, with $V_A = 2.18\,10^7$ cm s^{-1} the *Alfven velocity*, distributed inside a box with characteristic length $L = 3\,10^{10}$ cm). We study numerically the relation of the acceleration time to the number of shock waves and the length of the acceleration region. We also estimate that less than 20% of the total energy of the 200 shock waves goes into the acceleration of particles.

Key words: the Sun: flares – shock waves – acceleration mechanisms

1. Introduction

Particle acceleration mechanisms in Astrophysics can be divided into three broad classes (a) Coherent acceleration (e.g. electromagnetic waves, double layers, laminar shock waves), (b) Stochastic acceleration (e.g. MHD or electrostatic turbulence), (c) Mixed acceleration (e.g. turbulent shock waves).

We proposed here a mixed acceleration process. We assume that N-randomly formed shock waves interact simultaneously with the tail of the ambient distribution function of particles. The details of the formation of the N-shocks is different in solar flares, extragalactic jets, or supernova remnants. We discuss briefly below the mechanism that generates an N-shocks environment in several Astrophysics objects.

(a) Solar flares: A large amount of observational evidence points in the direction that in solar flares the energy is released (1) on very short time scales, (2) on small scale lengths and (3) as a large number of explosive phenomena (see Vlahos et al. 1986; Vlahos 1989). Parker (1972) proposed initially that if the footpoints of the bipolar fields are subject to random shuffling and mixing, then tangential discontinuities (*current sheets*) are formed and the amplitude of each discontinuity increases with time. Eventually a point is reached where rapid reconnection of the magnetic field across the individual discontinuities destroys them as fast as they are created by the motion of the footpoints.

We expect theoretically, and the observations seem to confirm this expectation, that bipolar fields above the surface of the Sun are filled with small scale reconnection events, i.e. filled with nanoflares, microflares or flares, depending of the total energy released. The discontinuities arise when the field is subjected to continuous but complex deformation, so that magnetic lines of force are wound and wrapped about each other in complicated patterns (see Parker 1988; Moffat 1987; Low & Wolfson 1988). Haerendel (1987) proposed that the current in the solar atmosphere is concentrated in 10^5 *narrow tubes*, carrying current ≈ 10 A m^{-2}. The strongly inhomogeneous pressure distribution set up in the corona as the result of the reconnection in multiple narrow current sheets which can act as a generator for even more intense currents and enhanced localised heating.

Observational evidence for the fragmentation of the flare energy release has been found in particular in radio emissions. Milliseconds spikes can appear in solar flares in great numbers (Benz 1985), also in Type III bursts the fragmentation of the energy release can reach to 1000 or more electron beams injected along individual 'fibers' (Roelof & Pick 1989, Aschwanden et al. 1990). We propose here that the active region is full of fibers (see Fig. 1) that interact and form narrow current sheets which are explosively heated and form shock waves (Cargill et al. 1988). We study in this article the acceleration of particles inside an N-shock waves environment.

(b) Extragalactic jets: Large scale MHD flows will form highly non-linear structures as they propagate in inhomogeneous plasma. The non-linear waves can form many individual discontinuities inside the flow. In other words, it is possible to form an N-shock waves environment inside a highly turbulent flow (see Fig. 3 from Kochanek & Hawley 1990).

(c) Supernova Remnants: A large spherical explosion of a supernova, if it propagates through an inhomogeneous medium,

Send offprint requests to: L. Vlahos

© European Southern Observatory • Provided by the NASA Astrophysics Data System

'1991A&A...245..271A'

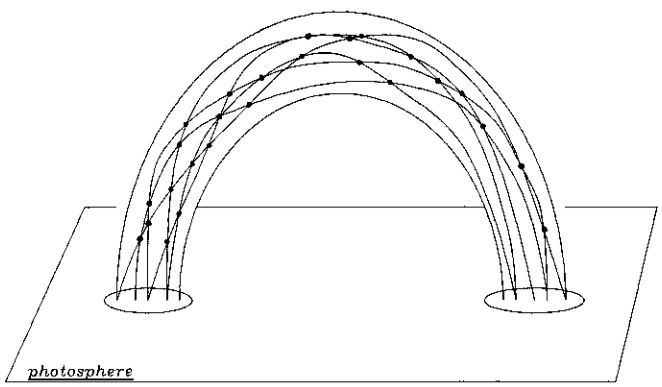

Fig. 1. A large scale loop is composed of thousands of small scale fibers. Hundreds of thousands of small scale explosions form a *'flare'*

can evolve away from the injection in a thick layer of randomly moving small scale discontinuities, or new explosions can appear inside the pre-existing wind driven bubble (see for example Tenorio-Tagle et al. 1990).

Toptyghin (1980) and Achterberg (1990) analysed the diffusive shock acceleration from an ensemble of shocks. Achterberg (1990) showed that if the shock waves are identical, as it may be the case in accreting flows, the spectrum is flattening as a result of the combined action of diffusive shock acceleration and expansion losses.

The numerical model and our analysis, using parameters typical for solar flares, are presented in the next section. In Sect. 3 we study the acceleration of a single particle inside the N-shocks environment and compare that mechanism to the Fermi acceleration process. Our numerical results, from the interaction of a large number of particles in the N-shocks environment, are presented in Sect. 4. The next section is concerning the energetics and scaling of the model and finally, in Sect. 6 we summarise our results and discuss the possible extensions of our model.

2. The model

We model an active region where many sudden releases of energy appear almost simultaneously and the plasma is heated locally. If the plasma parameter beta ($\beta = (8\pi\rho)/B^2$) exceeds unity, shock waves are formed and move away from the *hot spot* (Cargill et al. 1988). We use a *box* with characteristic length $L = 3\,10^{10}$ cm. Inside this *box* the plasma beta is $\beta = 5$ and the density $n_0 = 10^{10}$ cm^{-3}. The ambient magnetic field is $B_o = 10$ G and the *Alfven velocity* is $V_A = 2.18\,10^{11}\ B_o n_o^{-1/2} = 2.18\,10^7$ cm s^{-1}.

We assume that the shock waves travel with constant velocity V_{s_j} and their surface intersects the ambient magnetic field with different angles. When the shock escapes from the boundary of the *box* is considered *'lost'* from the acceleration region. The particles start with initial energy E_i and move along the ambient magnetic field. Their velocity is constant (U_p) between shocks but once they interact with the shock wave their energy changes (see next section) and continue their orbit upstream or downstream of the jth shock. Particles escaping from the *box* never return which means that we have not included in this model the effect of trapping. A typical overall trajectory of a particle inside an N-shock environment is shown in Fig. 2.

Each shock wave has a general geometry showing in Fig. 3. From the *Rankine-Hugoniot* conditions (Tidman & Krall 1971; Decker 1989), we evaluate the downstream parameters from the upstream ones. Typical values for the upstream parameters are: $\delta_1 = 0$, $\beta_1 = 5$, $U_1 = V_{s_j}$, $2.5 \le M_A \le 4$, $60° \le \theta_1 \le 86°$, $B_1 = 10$ G, where the V_{s_j} is the velocity of the jth shock wave, $M_A = U_1/V_A$ is the Alfvenic Mach number and the angle θ_1 is chosen randomly.

Since the angle between the ambient magnetic field and the shock normal is random, it is not important to follow the evolution of the pitch angle of the particle at the end of each encounter. In other words, we choose randomly the pitch angle of the particle at the end of each encounter.

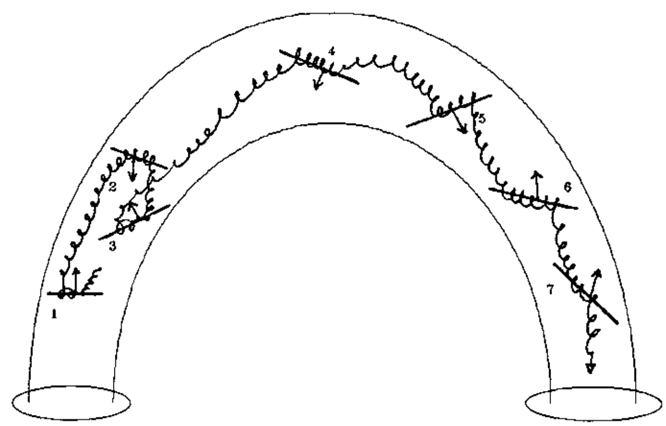

Fig. 2. A *'typical'* orbit of a particle interacting with N-shock waves. A particle drifts in shock wave 1, is reflected to shock wave 2, reflected again and continues to shock wave 3 etc. until it is transmitted by shock wave 7 and reached the chromosphere

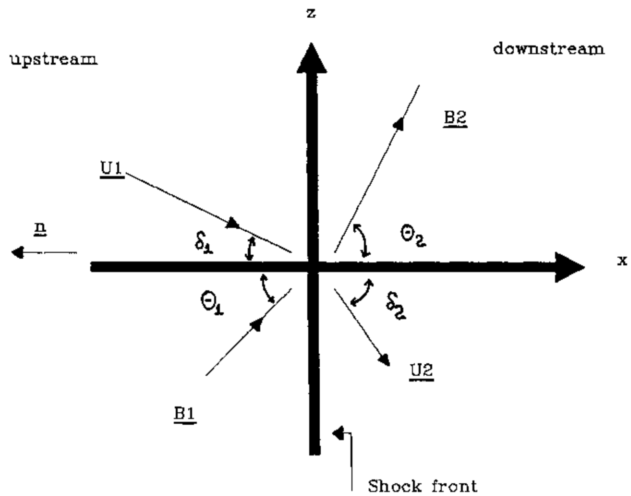

Fig. 3. The general geometry of the shock wave. The frame in which the shock is stationary is illustrated and the parameters for a constant and uniform flow are shown

3. Interaction of single particle with N-shocks

In the last section we presented the initialisation of the numerical technique that we are using. In this section we will present the results for the interaction of single particle with N-shock waves. First we will discuss the physical process on which the acceleration of the particle is based and at the end of this section we will compare our results with the *Fermi acceleration.*

© European Southern Observatory • Provided by the NASA Astrophysics Data System

'1991A&A...245..271A'

3.1. N-shock-single particle interaction

Particles can be accelerated in shock waves by either *drift* or *diffusive acceleration* mechanisms. In the diffusive mechanism, the particle is accelerated as it scatters back and forth across the shock front by the magnetic irregularities which exist in the upstream and in the downstream region (Toptyghin 1980; Drury 1982; Jokippii 1982). In the drift mechanism, the particle gains energy as it drifts along the electric field at the shock front (Sarris & Van Allen 1974; Webb et al. 1983; Armstrong et al. 1985; Decker 1989). In the case of the oblique shock wave with turbulence upstream and downstream, the acceleration of particles is a combination of the drift and the diffusive acceleration (Decker & Vlahos 1986).

The idea behind this study is to use an acceleration mechanism for the particle – shock interaction, which constitutes in our simulation an *'event'*. We choose the shock drift acceleration since it is the only one for which analytical expressions exist. Our results can be generalised when the shock waves are quasi-parallel or oblique with the presence of turbulents upstream or downstream. In this case the particle will trapped around the shock for longer time, moving upstream and downstream.

We are using the *adiabatic treatment* (Webb et al. 1983; Decker 1989), to calculate the energy changes of a particle interacting with the shock. The adiabatic theory is based on the fact that the magnetic moment of the particle is conserved in the frame of reference where the motional electric field is vanished. For the electron – shock wave interaction (Leroy & Mangeney 1984; Wu 1984; Krauss-Varban & Wu 1989) we neglect the electric potential in the shock transition as we assume that $E_i \gg e\Phi$, where E_i is the initial kinetic energy of the electron and Φ is the electric potential. The electrons are accelerated only by reflection at the shock front, the transmitted ones freely pass upstream or downstream without any energy change.

Using the numerical procedure described above, and assuming that the number of shock waves (N) is 100, we follow the energy of an ion with initial velocity $2\times V_{T_i}$, where $V_{T_i} \simeq 3.1\ 10^8$ cm s^{-1} is the thermal velocity of the ions (Fig. 4a), and $3\times V_{T_i}$ (Fig. 4b). For the same number of shock waves, we also follow the energy of an electron with initial velocity $2\times V_{T_e}$ (Fig. 4c) and $3\times V_{T_e}$ (Fig. 4d), with $V_{T_e} \simeq 4.2\ 10^9$ cm s^{-1} the thermal velocity of the electrons. The kinetic energy is normalised with the initial energy of the particle. The ions that are leaving the *box* have acquired energies $E \geq 80\ E_i$ in less than 5 s and the electrons are reaching energies $E \geq 25\ E_i$ in less than 1.5 s.

3.2. Fermi acceleration

Fermi (1949) proposed that the Galactic magnetic field was coupled to macroscopic plasma structures (*magnetic clouds*) which could move randomly, with constant velocity V_c and accelerate charged particles by means of collisions. It is well known that we can have two different types of collisions between a single magnetic cloud and a particle, the *head on collision* and the *overtaking collision*. At each *head on* collision the particle is accelerated and at the *overtaking* collision the particle is decelerated.

Assuming one spatial dimension and that in the cloud's rest frame the collision is elastic (since the cloud is massive), using a transformation between the cloud's rest frame and the observer's frame, we find that the change of the particle's energy (in the observer's frame) for one collision is given by the relation (see Longair 1981):

$$\Delta E = \pm 2E_i \gamma_V^2 \frac{V_c(V_i \pm V_c)}{c^2} \tag{1}$$

where E_i is the initial total energy of the particle, V_i is the velocity of the particle, V_c is the velocity of the cloud, $\Delta E = E_f - E_i$ is the difference of the energy due to collision with E_f the final total energy and γ_V is the *Lorentz* factor $\gamma_V = (1-(V_c^2/c^2))^{-1/2}$, the plus sign is for *a head on* collision and the minus is for an *overtaking* one.

We replace the shock waves inside the *box* with magnetic clouds with the same characteristic velocity and length as the shock waves. At each encounter of the particle with one magnetic cloud we increase the energy according to Eq. (1). Assuming that there are 100 magnetic clouds present inside the *box*, the change of the kinetic energy of an ion with initial velocity $V_i = 2\times V_{T_i}$ and $3\times V_{T_i}$ versus time is shown in Fig. 5a and 5b. The energy is normalised with the initial kinetic energy of the particle. The particles reached in the end of their interaction energy $E \leq 11\ E_i$ in 130 s!

It is obvious that *Fermi acceleration* is a slower process in comparison to the shock acceleration, since the particle needs more time in order to escape from the boundaries of the box. We should also mention here that we have used the same initialisation of the environment (shock waves and magnetic clouds) which accelerates the particles. During the *Fermi process* the particle undergoes a large number of collisions with the clouds while in the *shock drift acceleration* the particle has a smaller number of encounters with the shock waves, gaining a large amount of energy at each encounter.

4. Acceleration inside an N-shocks environment

4.1. Numerical estimate

We assume that a distribution of particles interact with N-shock waves following the numerical scheme used in Sect. 2. We use, both for ions and electrons, a power law distribution of the form:

$$f_k(u) = A \times u^{-\beta} \qquad k = i, e \tag{2}$$

where $f_k(u)$ is the velocity distribution of the *k-species*, A and β are constants and u is the velocity normalised to V_{T_k}, with $V_{T_i} = 3.1\ 10^8$ cm s^{-1} and $V_{T_e} = 4.2\ 10^9$ cm s^{-1} for the case of ions and electrons respectively.

Using $A \approx 7\ 10^4$ and $\beta \approx 4$ we find that the number of particles with velocity $u = 2V_{T_k}$ is $f_k(2V_{T_k}) \approx 4000$, $f_k(u = 3V_{T_k}) \approx 800$, $f_k(u = 4V_{T_k}) \approx 200$ and $f_k(u = 5V_{T_k}) \approx 100$ particles. For each of the four different velocities $u = 2, 3, 4, 5\times V_{T_k}$ we initialise 100 particles and calculate their final energy when they escape from the *box*, then we weighted our results (e.g. each particle with initial velocity $u = 2V_{T_k}$ is weighted with a factor 40 etc.) in order to find the energy distribution.

In Fig. 6 we show our results from the interaction of a distribution of particles with 200 shock waves. We plot the $f_k(E)$ vs (E/E_{N_k}), where $f_k(E)$ is the number of particles, $E_{N_i} = 200$ KeV for the ions (Fig. 6a) and $E_{N_e} = 20$ KeV for the electrons (Fig. 6b). Our results can be fit to a distribution:

$$f_k(E) = N_o \times \exp\left(-b_k \frac{E}{E_{N_k}}\right) \qquad k = i, e \tag{3}$$

© European Southern Observatory • Provided by the NASA Astrophysics Data System

'1991A&A...245..271A'

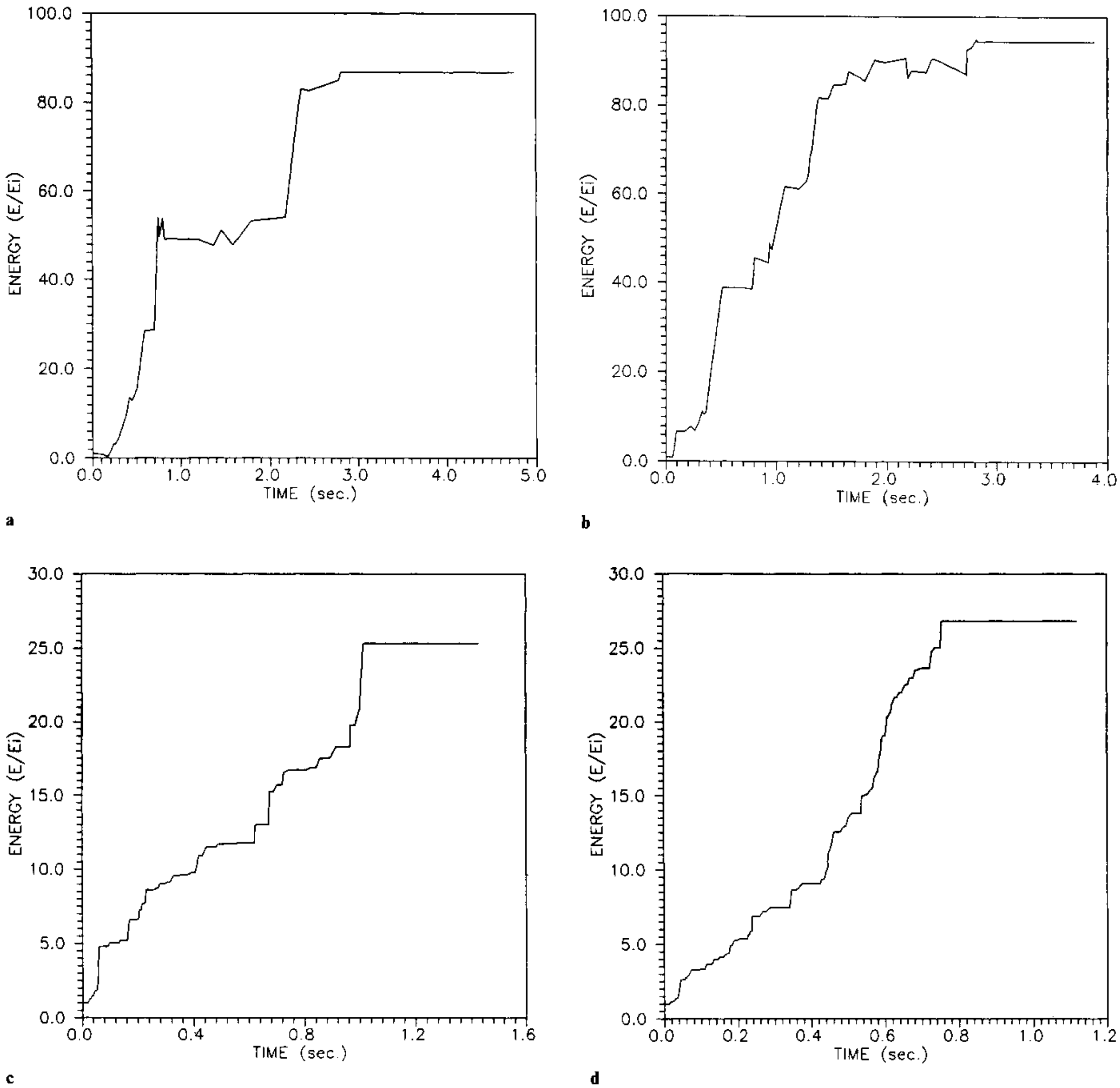

Fig. 4a–d. Kinetic energy variation versus time, for a single particle which interacts with $N=100$ shock waves. The energy is normalised with E_i and the time is in seconds. **a** Ion with $E_i=200$ KeV, **b** ion with $E_i=450$ KeV, **c** electron with $E_i=20$ KeV, **d** electron with $E_i=50$ KeV

where $b_i \simeq 1.5\,10^{-2}$ for the ions and $b_e \simeq 2.5\,10^{-2}$ for the electrons. From the Eq. (3) we find that the energy distribution of the particles is of the general form:

$$f_k(E) \approx \exp\left(-\frac{E}{E_{T_k}}\right) \quad k=i,\, e \tag{4}$$

with $E_{T_i} \simeq 13$ MeV for the ions and $E_{T_e} \simeq 1$ MeV for the electrons. In other words, the N-shock acceleration seems to produce a super-hot component for the ions with '*temperature*' $E \simeq 13$ MeV in less than 5 s and for the electrons with $E \simeq 1$ MeV in less than 1.5 s when $N=200$ and $L=3\,10^{10}$ cm.

4.2. *Analytical estimate*

Vas'kov et al. (1983) studied analytically the acceleration of electrons under the action of a localised E-field (*caviton*) produced by an electromagnetic wave in the region of an inhomogeneous plasma. It was shown that Coulomb collisions enabled the electrons to transverse the resonance region many times and resulted a significant acceleration of the electrons.

They consider a plasma that is weakly inhomogeneous along the z-axis and the resonance point is at $z_r=0$. The particles are accelerated at the layer z_r, the thickness of the accelerated layer is much smaller than the mean free path of the electron. The upper

© European Southern Observatory • Provided by the NASA Astrophysics Data System

'1991A&A...245..271A'

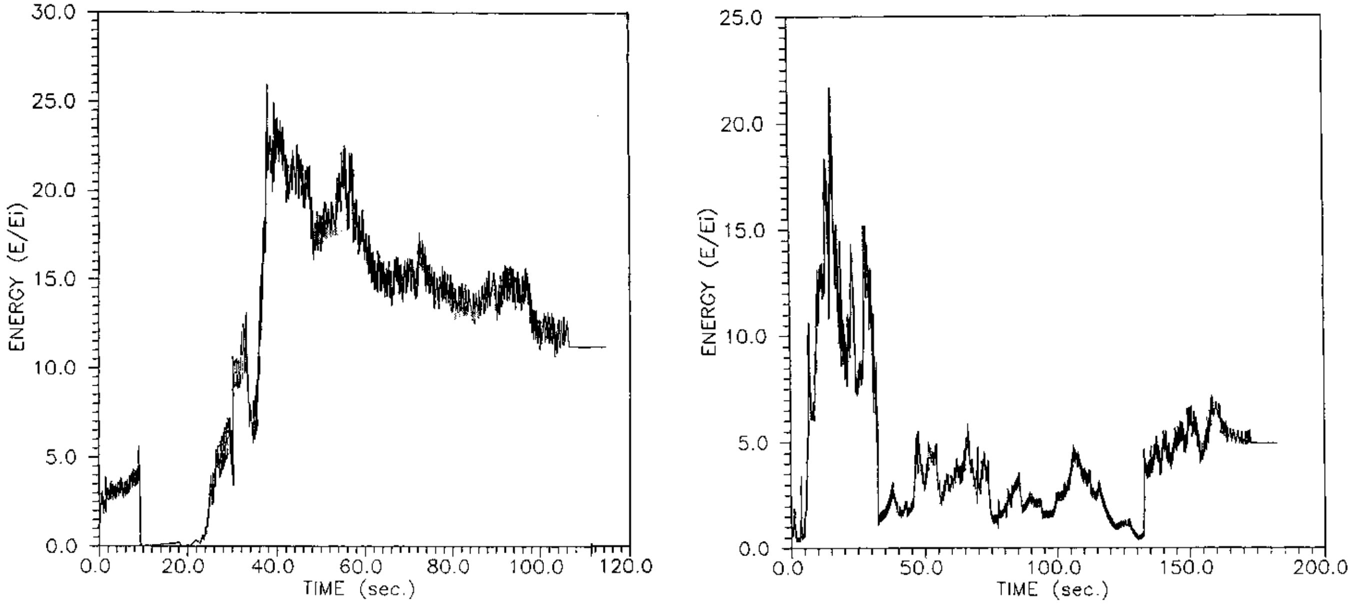

Fig. 5a and b. The same as in Fig. 4, but for Fermi acceleration of a single ion which interacts with $N=100$ magnetic clouds. **a** With $E_i=200$ KeV, **b** with $E_i=450$ KeV

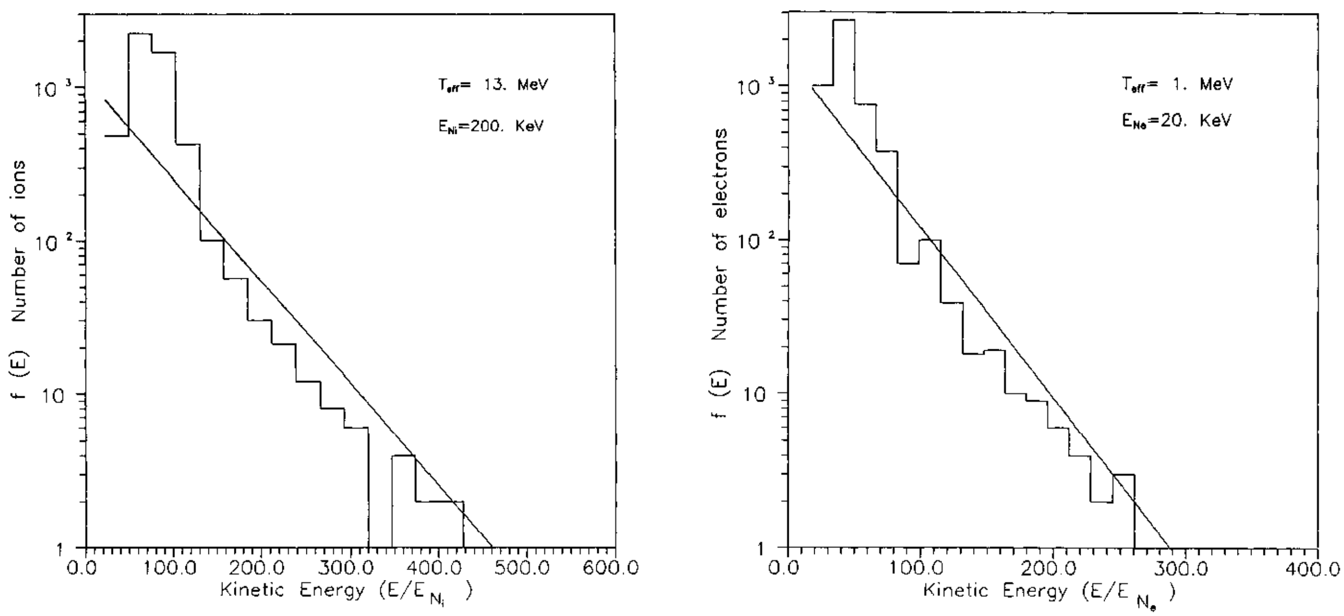

Fig. 6a and b. The final kinetic energy distribution of 5100 particles after their interactions with $N=200$ shock waves. The number of particles $f_k(E)$ versus the kinetic energy is illustrated, the energy is normalised with E_{N_k}. **a** Ions, with initial energy $E_{N_i}=200$ KeV, **b** electrons, with initial energy $E_{N_e}=20$ KeV

$(z>0)$ and lower $(z<0)$ parts of the plasma, are separated by the accelerating layer. The collisions play an important role since they reflect the particles back to the acceleration region.

We can solve the free streaming equation:

$$\frac{\partial f}{\partial t}+\mu v\frac{\partial f}{\partial z}=-S \tag{5}$$

where $f=f(t, E, \mu, z)$ is the electron distribution function. It depends on the time t, the coordinate z, the electron energy E and the angle θ between the direction of the velocity and z-axis, furthermore $\mu=\cos\theta$ and $v=(2E/m)^{1/2}$ and S is the collision integral. Since the E-field is localised at $z=0$, in Eq. (5) we are going to ignore the change of energy at the acceleration layer and solve analytically the motion of the particle at $z=0$ e.g.

© European Southern Observatory • Provided by the NASA Astrophysics Data System

'1991A&A...245..271A'

$$\frac{\partial v_{\|}}{\partial t}+\frac{1}{2}\frac{\partial v_{\|}^2}{\partial z}=-\frac{e}{m}E(z,t). \tag{6}$$

Assuming that the $\boldsymbol{E}$-field is localised with amplitude E_o and length α, we can estimate the maximum energy change in one crossing, $\Delta E_m = eE_o\alpha$. After determining the electron energy increment ΔE, following the passage of the acceleration layer, we find the corresponding change of the average distribution. The $f(E-\Delta E)$ energy distribution is now used in Eq. (5) to follow its evolution upstream ($z>0$) or downstream ($z<0$). Solving the Eq. (5) by using the above assumptions Vas'kov et al. found that the distribution function of the accelerated electrons had the form:

$$f(E)\approx \exp\left(-\frac{E}{T_{\rm eff}}\right) \tag{7}$$

where the $T_{\rm eff}$ determines the new *effective temperature*, defined by the relation:

$$T_{\rm eff}\simeq\frac{3^{1/4}}{2\sqrt{2}}\langle\Delta E\rangle \tag{8}$$

where $\langle\Delta E\rangle$ is the average increment of the energy in the acceleration layer. They found also that if there are N cavitons present and assuming that the maximum increment of energy of the particle at each caviton is ΔE_m, then the maximum *effective temperature* is defined by the relation:

$$T_{{\rm eff}_m}\simeq\frac{3^{1/4}}{2\sqrt{2}}\sqrt{\frac{N}{2}}\,\Delta E_m. \tag{9}$$

Shock drift acceleration by N randomly moving shock waves is almost identical problem with the one studied above since; (1) the acceleration is localised at the shock front, (2) the energy gained or lost by the particle is proportional to the distance particles drift along the shock surface, (3) the particles do not return to the same shock by collisions but interact with different shock waves before escaping the acceleration volume. The only difference with the caviton problem is that the $\langle\Delta E\rangle$ used in Eq. (8) should be estimated numerically since, many random factors control the drift distance along the shock front.

Applying the analytical results in our case, the average increment of the energy of the particles, after their interaction with $N=200$ shock waves, is $\langle\Delta E\rangle_i\simeq 27.5$ MeV and $\langle\Delta E\rangle_e\simeq 2$ MeV. Using Eq. (8) we find that the *effective temperature* of the electrons is $T_{{\rm eff}_e}\simeq 1$ MeV and for the ions $T_{{\rm eff}_i}\simeq 13$ MeV. These values are identical with the ones estimated numerically in Sect. 4.1

Other important differences between the analytical results and the numerical estimates presented here are: (1) the analytical solution of the kinetic equation is, a study state solution, (2) the size of the acceleration volume depends strongly on the collision frequency of the particles. In other words, the estimates of the acceleration time and the role of the length of the acceleration volume on the distribution of the energetic particles can be done only numerically.

5. On the energetics and scaling of the model

In the last section we showed that $N=200$ shock waves, moving with mean velocity $V_s\simeq 7\,10^7$ cm s^{-1} and randomly placed inside the acceleration volume (L^3), will "energise" a large percentage of particles ($n_t\geq 10^{-2}n_o$) which have velocities $\geq 2\times V_{T_k}$. This interaction produces a super-hot component for the particles with effective temperature $T_{{\rm eff}_k}$. In this section we are going to estimate the percentage of the energy carried by the shock waves, that goes to the accelerated particles (ions and electrons).

It is well known that the total energy of a single shock wave is equal to the sum of the *Kinetic*, *Magnetic* and *Thermal* energy. For the parameters used in our model and assuming that the density of ions is equal to that of electrons, we find that the *Kinetic energy density* for a shock wave is $W_K\simeq(1/2)n_o m_i V_s^2\simeq 2.55\,10^{19}$ eVm^{-3}, the *Magnetic energy density* is $W_M\simeq(B^2/8\pi)\simeq 2.48\,10^{18}$ eVm^{-3} and the *Thermal energy density* is $W_T=\beta\times W_M\simeq 1.24\,10^{19}$ eVm^{-3}. For $N=200$ shock waves the total energy density is:

$$W_{\rm tot}=N\times(W_K+W_M+W_T)\simeq 8.08\,10^{21}\,{\rm eVm}^{-3}. \tag{10}$$

The energy density of the accelerated ions is:

$$W_i\simeq n_t T_{{\rm eff}_i}\simeq 1.3\,10^{21}\,{\rm eVm}^{-3} \tag{11}$$

and of electrons:

$$W_e\simeq n_t T_{{\rm eff}_e}\simeq 1\,10^{20}\,{\rm eVm}^{-3} \tag{12}$$

using $T_{{\rm eff}_i}=13$ MeV, $T_{{\rm eff}_e}=1$ MeV.

Assuming that the 'length' of the acceleration volume energised by each shock wave is $\simeq V_s t_l$, where $t_l\approx 1-5$ s is the life time of the shock wave, we find that the energy accumulated in the shock waves is $\approx 10^{29}$ erg, which is almost 1% of the total energy of the flare. Finally from the Eqs. (10)–(12) we find that the fraction of the total energy of the shocks that goes to the accelerated ions is:

$$P_i=\frac{W_i}{W_{\rm tot}}\simeq 16\,10^{-2} \tag{13}$$

and that of electrons is:

$$P_e=\frac{W_e}{W_{\rm tot}}\simeq 1.2\,10^{-2}. \tag{14}$$

It is obvious from Eqs. (13) and (14) that less of the 20% of the total energy carried by the shock waves goes to the acceleration of the particles (ions and electrons). The rest of the energy released goes to the heating of the acceleration volume.

An important diagnostic for the validity of our acceleration model is the electron-proton ratio energised in a flare. Using the distributions given by Eq. (7) we estimate the electron-proton ratio (n_{e-p}) for energy above 30 MeV,

$$n_{e-p}=\frac{n_o A_e\int_{30\,{\rm MeV}}^{\infty} f_e(E)\,{\rm d}E}{n_o A_i\int_{30\,{\rm MeV}}^{\infty} f_i(E)\,{\rm d}E}\simeq e^{-30[(1/T_{{\rm eff}_e})-(1/T_{{\rm eff}_i})]} \tag{15}$$

where A_e and A_i are the normalised factors of the distributions. If we combine the Eqs. (8)–(9) with the Eq. (15), we find that n_{e-p} depends on the number of shock waves. Assuming that the number of shocks present in the acceleration volume is $N\approx 4000$, the electron-proton ratio is $n_{e-p}\approx 10^{-3}$. This estimate agrees well with the result presented by Ramaty & Murphy (1987).

Using our numerical results we can make the following observations:

(1) The acceleration time is related to the characteristic dimensions of the acceleration region (see Fig. 7).

© European Southern Observatory • Provided by the NASA Astrophysics Data System

'1991A&A...245..271A'

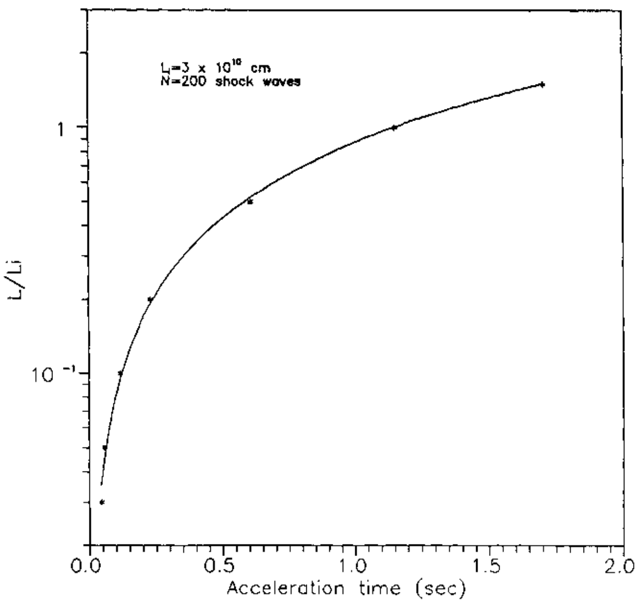

Fig. 7. The dependence of the acceleration time of the particles with the characteristic length of the acceleration volume, as the number of shock waves is $N=200$. ($L_i = 3\,10^{10}$ cm)

(2) As the number of shock waves increases inside an acceleration region of a constant length, the acceleration time remains almost constant (see Fig. 8).

(3) The super-thermal temperature is proportional to the square root of the number of shocks (see Eq. (9)). It is obvious that if the number of shocks waves increases by a factor 100–1000 inside the same volume we can reach energies up to GeV for protons and 50–100 MeV for electrons without radical changes of the acceleration time.

(4) The number of high energy particles which can be produce from the interaction with a constant number of shock waves is strongly dependent to the length of the acceleration volume (see Fig. 9).

6. Summary and conclusions

Solar flares have been modelled so far as a single large explosion inside a loop, during the interaction of two arcades, or above an erupting filament etc. In this scenario there was only *one* "Energy Release Site" and particles were heated or/and accelerated in a *single* volume by a *single* explosion. Particle acceleration was modelled on basis of this hypotheses assuming that large scale electric fields, large scale shock waves or MHD turbulence exist. The main question that has remained unanswered so far was the way these structures were formed and how their strength is determined (e.g. How strong is the electric field and what is its spatial extend? What is the level of the MHD wave activity and how sets in? etc.). In this article we present a natural way for the formation of shock waves, assuming that small scale explosions or a large number of discontinuities are formed above active regions, in Jet flows, or during Supernovae explosions.

In our study we focus on the short time scale evolution of the N-shock wave-particle interaction. We have completely avoided questions related to energy loss by shock wave propagation or shock-shock collisions (Cargill et al. 1986; Cargill & Goodrich 1987; Cargill 1991). By including these effects in our model we will find that most of the energy released by the '*thermal*' explosions will return to thermal energy through the shock-shock interactions.

Starting with an energy release volume with characteristic length L, two important parameters, the mean free-path for the shock-shock collisions (λ_{s-s}) and the mean free-path of the particle-shock collision (λ_{p-s}), will define if the flare will be

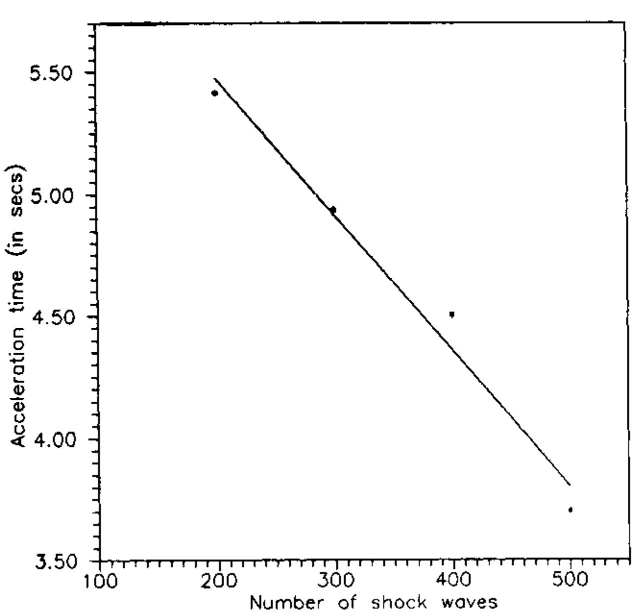

Fig. 8. The dependence of the acceleration time of the particles with the number of shock waves, as the characteristic dimension of the acceleration region is constant ($L = 3\,10^{10}$ cm)

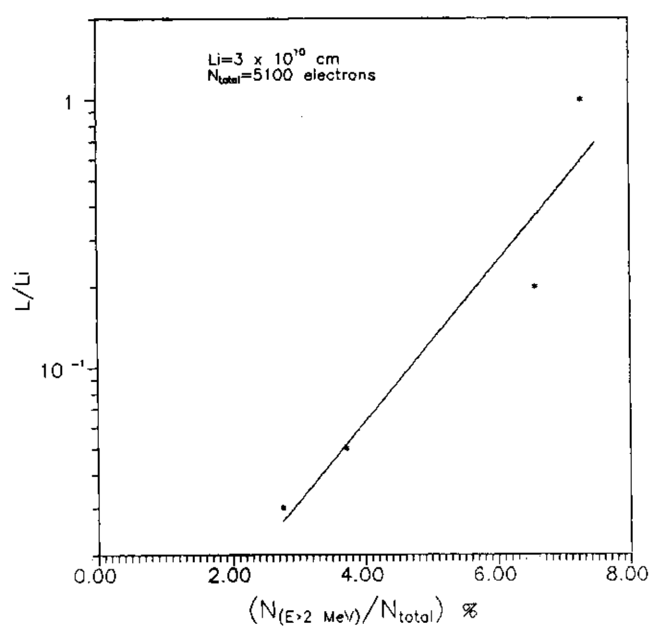

Fig. 9. The dependence of the high energy electrons ($E \geq 2$ MeV) with the characteristic dimension of the acceleration region, when there are 200 shock waves and the total number of electrons is $N_{\rm total} = 5100$

© European Southern Observatory • Provided by the NASA Astrophysics Data System

'1991A&A...245..271A'

'*thermal*' (X-ray emission is primarily due to a thermal distribution) or '*non-thermal*' (the X-ray emission is primarily due to the super-thermal tail). If $\lambda_{s-s} \ll \lambda_{p-s}$ the shock-shock collisions will be more frequent and will transfer most of the energy released locally into a large scale heating. In the opposite case $\lambda_{s-s} \gg \lambda_{p-s}$ (studied here), the non-thermal tail will play the dominant role since the shocks will have plenty of time to accelerate particles before shock-shock interactions dominate over shock-particle interactions. Finally when $\lambda_{s-s} \approx \lambda_{p-s}$ both heating and acceleration are equally important.

We can now study the flare phenomenon from the pre-flare to the post flare evolution as an evolution of a number of N local explosions and the parameter $\lambda_{p-s}/\lambda_{s-s}$. We can start with a few explosions and $\lambda_{p-s}(\ll \lambda_{s-s})$ dominant during the pre-impulsive phase, then during the impulsive phase N increases dramatically inside a compact volume and $\lambda_{p-s} \approx \lambda_{s-s}$ and during the post impulsive phase N reduces, the energy release volume increases and $\lambda_{p-s} \gg \lambda_{s-s}$.

Finally we showed in this article that the interaction of a distribution of particles (ions and electrons) with the N-shock waves under the assumptions discussed above produces a super-hot component for the particles. Our main conclusions are:

(1) For the case of $N=200$ shock waves and for characteristics of solar flares, that we can define a new *effective temperature* for the final distribution, with $E_{T_i} \simeq 13$ MeV for the ions and $E_{T_e} \simeq 1$ MeV for the electrons. The effective temperature estimated from our numerical work agrees well with the analytical work of Vas'kov et al. (1983). We show also that ions with initial kinetic energy 200 KeV $\leq E_i \leq 1.2$ MeV are accelerated up to $20-60$ MeV in less than 5 s and electrons with initial energy range 20 KeV $\leq E_i \leq 200$ KeV are accelerated up to 5 MeV in less than 1.5 s.

(2) Only 20% of the energy carried by the shock waves goes to particle acceleration.

(3) The acceleration time can become as small as 0.1 s for $L=3\,10^8$ cm and it is independent of the number of shock waves present. In other words, increasing the number of shock waves inside an acceleration volume we can reach very high energies in a very short time scales.

(4) The electron-proton ratio estimated for $N \approx 4000$ shock waves agrees with the observational results.

In summary we believe that this acceleration scheme satisfies most of the requirements for the acceleration of protons and electrons in solar flares.

Acknowledgements. The present research is a part of the Ph.D. thesis of one of the authors (A.A.). Also A.A. acknowledges the support of the European Astrophysics Doctoral Network and the Max Planck Institut fur Extraterrestrische Physik (MPE) for his 6 months stay in Garching, where a part of the computational work reported here was performed. Authors would like to thank Prof. E.N. Parker for his comments and Dr. P.J. Cargill for useful discussions.

References

Achterberg A., 1990, A&A 231, 251
Aschwanden M.J., Benz A.O., Schwartz R.A., Lin R.P., Pelling R.M., Stehling W., 1990, Sol. Phys. 130, 39
Armstrong T.P., Pesses M.E., Decker R.B., 1985, in: Collisionless shocks in the Heliosphere: Reviews of Current Research, eds. B.T. Tsurutani, R.G. Stone, *Geoph. Mongr. Ser.* 35, 271
Benz A.O., 1985, Solar Phys. 96, 357
Cargill P.J., 1991, ApJ (in press)
Cargill P.J., Goodrich C.C., Papadopoulos K., 1986, Phys. Rev. Lett. 56, 1988
Cargill P.J., Goodrich C.C., 1987, Phys. Fluids 30, 2504
Cargill P.J., Goodrich C.C., Vlahos L., 1988, A&A 189, 254
Decker R.B., 1989, Space Sci. Rev. 48, 195
Decker R.B., Vlahos L., 1986, ApJ 306, 710
Drury L.O'C., 1983, Rep. Prog. Phys. 46, 973
Fermi E., 1949, Phys. Rev. 75, No. 8, 1169
Jokippii J.R., 1982, ApJ 255, 716
Haerendel G., 1987, Proc. 21st ESLAB Symposium, Norway, ESA SP-275
Krauss-Varban D., Wu C.S., 1989, J. Geophys. Res. 94, 15367
Kochaneck C.S., Hawley J.F., 1990, ApJ 350, 561
Leroy M.M., Mangeney A., 1984, Annal. Geophys. 2, 449
Longair M.S., 1981, High energy Astrophysics, Cambridge University Press, Cambridge
Low B.C., Wolfson R., 1988, ApJ 324, 574
Moffat H.K., 1987, in: Advances in Turbulence, eds. G. Comte-Bellot, J. Matieu, Springer, Berlin Heidelberg New York, p. 240
Parker E.N., 1972, ApJ 174, 499
Parker E.N., 1988, ApJ 330, 474
Ramaty R., Murphy R.J., 1987, Space Sci. Rev. 45, 213
Roelof E.C., Pick M., 1989, A&A 210, 417
Sarris E.T., Van Allen J.A., 1974, J. Geophys. Res. 79, 4157
Tenorio-Tagle G., Bodenheimer P., Franco J., Rozyczka P.J., 1990, MNRAS 244, 563
Tidman D.A., Krall N.A., 1971, Shock waves in collisionless plasmas, Wiley, New York
Toptyghin I.N., 1980, Space Sci. Rev. 26, 157
Webb G.M., Axford W.I., Terasawa T., 1983, ApJ 270, 537
Wu C.S., 1984, J. Geophys. Res. 89, 8857
Vas'kov V.V., Gurevich A.V., Dimant Ya.S., 1983, Sov. Phys. JETP 52, 310
Vlahos L., Machado M.E., Ramaty R., Murphy R.J., Alissandrakis C., Bai T., Bactchelor D., Benz A.O., Chupp E., Ellison D., Evenson P., Forrest D.J., Holman G., Kane S.R., Kaufmann P., Kundu M.R., Lin R.P., Mackinnon A., Nakajima H., Pesses M., Pick M., Ryan J., Schwartz R.A., Smith D.F., Trottet G., Tsuneta S., Van Hoven G., 1986, Energetic Phenomena on the Sun, NASA CP-2439, p. 2–1
Vlahos L., 1989, Solar Phys. 121, 431

© European Southern Observatory • Provided by the NASA Astrophysics Data System